




Cell death modes are specified by the crosstalk dynamics within pyroptotic and apoptotic signaling

Cite as: Chaos 31, 093103 (2021); <https://doi.org/10.1063/5.0059433>

Submitted: 09 June 2021 . Accepted: 17 August 2021 . Published Online: 08 September 2021

Zhiyong Yin, Pei-pei Zhang, Fei Xu, Zhilong Liu, Ligang Zhu, Jun Jin,  Hong Qi,  Jianwei Shuai,  Xiang Li, et al.



View Online



Export Citation



CrossMark

Scilight

Summaries of the latest breakthroughs
in the **physical sciences**



Cell death modes are specified by the crosstalk dynamics within pyroptotic and apoptotic signaling

Cite as: Chaos 31, 093103 (2021); doi: 10.1063/5.0059433

Submitted: 9 June 2021 · Accepted: 17 August 2021 ·

Published Online: 8 September 2021






View Online



Export Citation



CrossMark

Zhiyong Yin,¹ Pei-pei Zhang,² Fei Xu,¹ Zhilong Liu,¹ Ligang Zhu,¹ Jun Jin,¹ Hong Qi,³  Jianwei Shuai,^{1,2,4,a)} 
and Xiang Li^{1,2,a)} 

AFFILIATIONS

¹Department of Physics, Xiamen University, Xiamen 361005, China

²State Key Laboratory of Cellular Stress Biology, School of Life Sciences, Innovation Center for Cell Signaling Network, Xiamen University, Xiamen 361102, China

³Complex Systems Research Center, Shanxi University, Taiyuan 030006, China

⁴National Institute for Data Science in Health and Medicine, Xiamen University, Xiamen 361102, China

^{a)}Authors to whom correspondence should be addressed: jianweishuai@xmu.edu.cn and xianglibp@xmu.edu.cn

ABSTRACT

The crosstalk between pyroptosis and apoptosis pathways plays crucial roles in homeostasis, cancer, and other pathologies. However, its molecular regulatory mechanisms for cell death decision-making remain to be elucidated. Based on the recent experimental studies, we developed a core regulatory network model of the crosstalk between pyroptosis and apoptosis pathways. Sensitivity analysis and bifurcation analysis were performed to assess the death mode switching of the network. Both the approaches determined that only the level of caspase-1 or gasdermin D (GSDMD) has the potential to individually change death modes. The decrease of caspase-1 or GSDMD switches cell death from pyroptosis to apoptosis. Seven biochemical reactions among the 21 reactions in total that are essential for determining cell death modes are identified by using sensitivity analysis. While with bifurcation analysis of state transitions, nine reactions are suggested to be able to efficiently switch death modes. Monostability, bistability, and tristability are observed under different conditions. We found that only the reaction that caspase-1 activation induced by stimuli can trigger tristability. Six and two of the nine reactions are identified to be able to induce bistability and monostability, respectively. Moreover, the concurrence of pyroptosis and apoptosis is observed not only within proper bistable ranges, but also within tristable ranges, implying two potentially distinct regulatory mechanisms. Taken together, this work sheds new light on the crosstalk between pyroptosis and apoptosis and uncovers the regulatory mechanisms of various stable state transitions, which play important roles for the development of potential control strategies for disease prevention and treatment.

Published under an exclusive license by AIP Publishing. <https://doi.org/10.1063/5.0059433>

Most recently, extensive studies have been focused on elucidating the molecular mechanisms of pyroptosis, which is a new procedural and inflammatory death. Pyroptosis is related to various diseases, such as auto-immune disease, cardiovascular disease, metabolic disease, and malignant tumors. With this paper, we aim to explore the regulatory mechanisms of how the crosstalk dynamics between pyroptotic and apoptotic signaling generate specific cell fate decisions. To this end, we build a core regulatory network model that is quantitatively supported by experimental data. We systematically present how various states of death modes, i.e., monostability, bistability, and tristability, are determined by the components. Caspase-1, GSDMD, and nine

biochemical reactions are identified that can efficiently switch cell death modes. Moreover, the concurrence of pyroptosis and apoptosis is predicted to be observed under certain circumstances. These results provide possible clues to guide the development for the prevention and treatment of pyroptosis-related diseases.

INTRODUCTION

Pyroptosis, a form of programmed cell death, is accompanied by cell swelling, membrane rupture, and lysis, which ultimately causes massive release of cellular contents and induces

inflammation.^{1,2} Pyroptosis exerts a significant role in the clearance of infectious agents by releasing the surviving intracellular bacteria for neutrophil-mediated killing.³ However, pyroptosis is also related to various diseases, such as auto-immune disease, cardiovascular disease, metabolic disease, and malignant tumors. Understanding the regulation mechanism of pyroptosis is, therefore, urgent for disease prevention and treatment.⁴

Pyroptosis is triggered by the inflammasome, which is a cytosolic macromolecular signaling complex that regulates host immune responses to invading pathogens and danger signals.⁵ The formation of the inflammasome is initiated by cytosolic pattern recognition receptors, which are innate immune sensors to recognize pathogen-associated molecular patterns (PAMPs) or danger-associated molecular patterns (DAMPs), including anthrax toxin, bacterial flagellin, double-stranded DNA, toll-like receptors, and so on.⁶ Over the past ten years, great progress has been made on the molecular mechanisms of pyroptosis in response to diverse PAMPs or DAMPs.⁷ Pyroptosis was primarily recognized as a pro-inflammatory pathway resulting from the study of caspase-1-mediated macrophage death.⁸ In 2015, gasdermin D (GSDMD) was identified as the cleavage target for caspase-1 and the executioner of pyroptosis, which is landmark progress for this research field.^{9–11} Recent studies widely reported that pyroptosis critically depends on the formation of plasma membrane pores by members of the gasdermin family.^{12,13} Besides, more and more pyroptosis-related caspases were identified successively.¹⁴

The emerging connectivity of different types of cell death pathways and its physiological implications are the focus of current research.^{15,16} The crosstalk between pyroptosis and apoptosis pathways has attracted much attention very recently. A large quantity of experiments reported that deficient of GSDMD or caspase-1 could switch cell death modes from pyroptosis to apoptosis.^{9,17} Taabazuing *et al.* found that caspase-1 not only cleaves GSDMD, but also activates the apoptosis effector, caspase-3, with a comparatively slow kinetic. In addition, the caspase-1-activated caspase-3 can cleave GSDMD during apoptosis to eliminate the ability of cells to undergo pyroptosis, indicating that the role of caspase-1 in pyroptosis is bidirectional.¹⁸ In 2017, Rogers *et al.* found that the activated caspase-3 can cleave gasdermin E (GSDME) to induce cell pyroptosis after caspase-3 successfully induces apoptosis.¹⁹ Their latest work showed that GSDME also targets the mitochondrial membrane, with concomitant release of cytochrome c and apoptosome formation.²⁰ Moreover, Sarhan *et al.* and Orning *et al.* found that caspase-8 is capable of inducing the cleavage of both GSDMD and GSDME to ignite pyroptosis during certain types of extrinsic and intrinsic apoptosis.^{21,22} Chen *et al.* further corroborated that caspase-8 can suppress pyroptosis in a manner of cleaving GSDMD of aspartate-88 by caspase-3.²³

Besides the experimental studies, theoretical study is also a powerful approach to reveal the complicated regulatory mechanism of signaling pathways.^{24–26} Yet, as a newly identified death type, few studies have been performed to systematically explore the regulatory mechanisms of pyroptosis pathway, among which a fundamental question is how the crosstalk between pyroptotic and apoptotic signaling generates the specific cell fate decisions. Motivated by this, we thus built a core regulatory network model based on the recently experimental data to discuss the crosstalk dynamics between pyroptosis and apoptosis pathways.

Both sensitivity analysis and bifurcation analysis were performed to address the underlying switching mechanisms, providing possible therapeutic strategies for controlling various death modes.

RESULTS

Data-driven modeling of the crosstalk between pyroptotic and apoptotic signaling

To investigate the dynamics of the cell death decision-making network, a coarse-grained model is developed based on our current understanding of the crosstalk between pyroptotic and apoptotic signaling. The detailed biological background of the crosstalk (Fig. S1 in the [supplementary material](#)) and the reason why the coarse-grained method is employed in our study can be found in Appendix A in the [supplementary material](#). The simplified network is shown in Fig. 1(a), which comprises five key constituents, i.e., caspase-1, caspase-8, GSDMD, caspase-9, and caspase-3. Upon stimulation, caspase-1, a multi-functional protein, is recruited into the inflammasome and then activated. The activated caspase-1 can cleave GSDMD to trigger pyroptosis. Meanwhile, caspase-1 can activate caspase-9, which is an essential part of apoptosome for inducing the caspase-3-mediated apoptosis.¹⁷ The cleaved GSDMD can also promote the activation of caspase-1.²⁷ It is also widely reported that caspase-1 can directly activate caspase-3 with slow dynamics.^{17,18} Moreover, although caspase-1 restricts the recruitment of caspase-8 into inflammasome, it can also activate caspase-8 directly.²⁸ The activated caspase-8/9 can further cleave the apoptosis effector, caspase-3. The cleaved caspase-3 also activates caspase-8/9, providing efficient positive feedback for apoptosis induction.^{29–31} Pyroptosis and apoptosis seem to compete with each other. The apoptosis effector caspase-3 suppresses pyroptosis through inhibiting GSDMD,¹⁸ while GSDMD can block apoptosis through strongly inhibiting the activation of caspase-8 by caspase-1, which is supported by the experiment that apoptosis occurs in GSDMD deficient cells.^{9–11} Besides, GSDMD can also limit the activation of caspase-3 by caspase-8/9.¹⁷

Based on the schematic network shown in Fig. 1(a), we constructed a corresponding model comprising five constituents, i.e., caspase-1 (C1), caspase-8 (C8), caspase-9 (C9), caspase-3 (C3), and GSDMD (GD). The death decision-making process of the system is described by five coupled ordinary differential equations (ODEs) presented below,

$$\begin{aligned} \frac{d[C1]}{dt} = & k_1 * ([C1_{tot}] - [C1]) * \frac{S^{n_1}}{S^{n_1} + j_{s1}^{n_1}} + k_{-1} \\ & * \frac{[GD]^{n_{14}}}{[GD]^{n_{14}} + j_{GD}^{n_{14}}} * ([C1_{tot}] - [C1]) - k_{dC1} * [C1], \quad (1) \end{aligned}$$

$$\begin{aligned} \frac{d[GD]}{dt} = & k_2 * \frac{[C1]^{n_2}}{[C1]^{n_2} + J_{C1}^{n_2}} * \frac{J_{C3i}^{n_3}}{J_{C3i}^{n_3} + [C3]^{n_3}} * ([GD_{tot}] - [GD]) \\ & - k_{dGD} * [GD], \quad (2) \end{aligned}$$

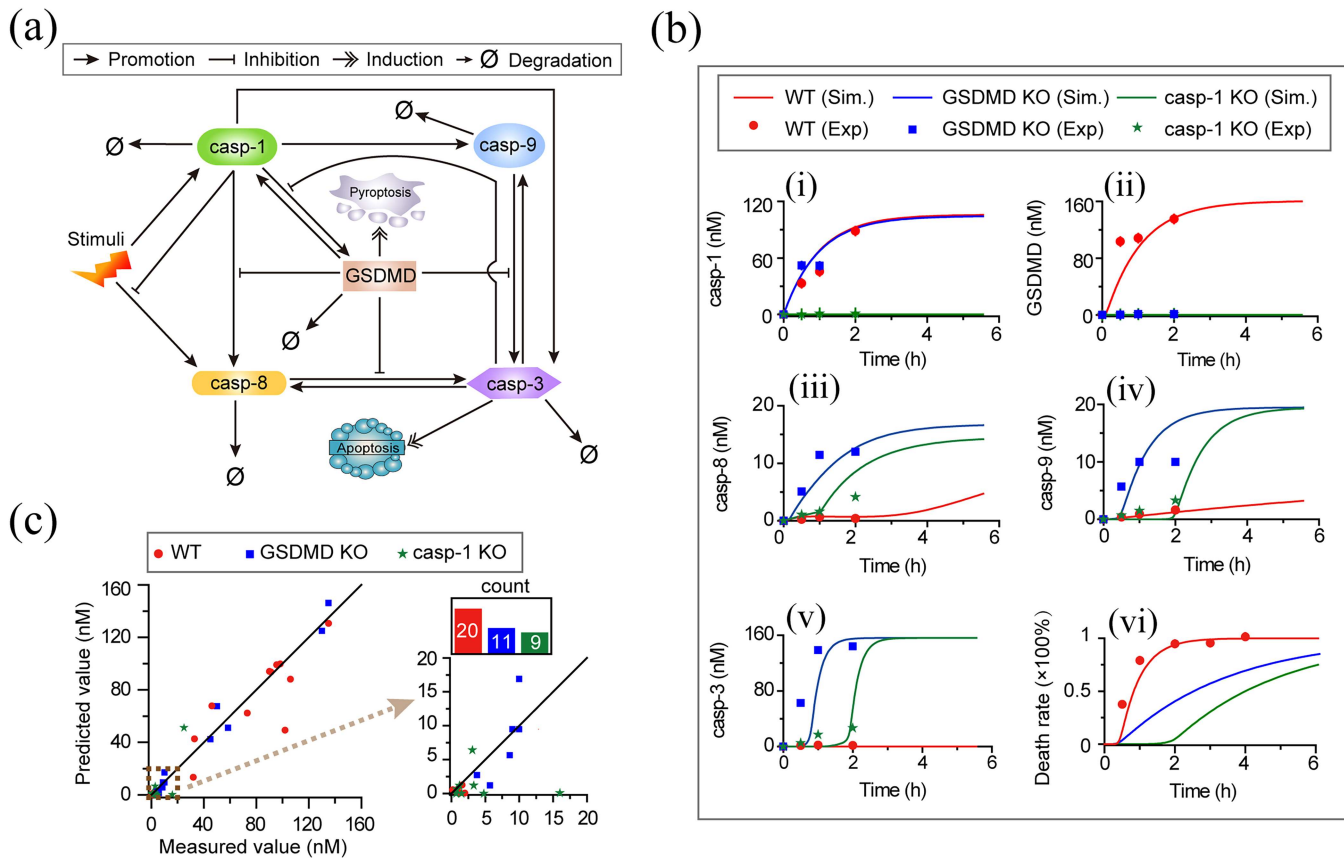


FIG. 1. Modeling the crosstalk between pyroptosis and apoptosis pathways. (a) The core regulatory network of pyroptosis and apoptosis pathways. The network contains five key constituents: caspase-1/3/8/9 and GSDMD. Caspase-3 and GSDMD are the effector proteins for inducing apoptosis and pyroptosis, respectively. (b) Comparison between experimental data (dots) and simulation results (lines) of the constituent time-course responses. The results of three different conditions are colored by red (wildtype, WT), blue (GSDMD knockout, GSDMD KO), and green (caspase-1 knockout, caspase-1 KO). (c) Scatter diagram of experimental data vs theoretical results. There are totally 20, 11, and 9 comparison results for the three conditions, respectively.

$$\frac{d[C9]}{dt} = k_3 * \frac{[C1]^{n_4}}{[C1]^{n_4} + J_{C1}^{n_4}} * ([C9_{tot}] - [C9]) + k_{C3} * \frac{[C3]^{n_5}}{[C3]^{n_5} + J_{C3}^{n_5}} * ([C9_{tot}] - [C9]) - k_{dC9} * [C9], \quad (3)$$

$$\frac{d[C8]}{dt} = k_4 * \frac{S^{n_6}}{S^{n_6} + j_{S2}^{n_6}} * \frac{j_{C1}^{n_7}}{j_{C1}^{n_7} + [C1]^{n_7}} * ([C8_{tot}] - [C8]) + \left(k_{C3} * \frac{[C3]^{n_8}}{[C3]^{n_8} + J_{C3}^{n_8}} + k_{-4} * \frac{[C1]^{n_{15}}}{[C1]^{n_{15}} + j_{15}^{n_{15}}} * \frac{j_{GD1}^{n_{16}}}{j_{GD1}^{n_{16}} + [GD]^{n_{16}}} \right) * ([C8_{tot}] - [C8]) - k_{dC8} * [C8], \quad (4)$$

$$\frac{d[C3]}{dt} = k_5 * \frac{[C9]^{n_{10}}}{[C9]^{n_{10}} + J_{C9}^{n_{10}}} * \frac{J_{GD}^{n_{11}}}{J_{GD}^{n_{11}} + [GD]^{n_{11}}} * ([C3_{tot}] - [C3]) + k_{C8} * \frac{[C8]^{n_{12}}}{[C8]^{n_{12}} + J_{C8}^{n_{12}}} * \frac{J_{GD}^{n_{13}}}{J_{GD}^{n_{13}} + [GD]^{n_{13}}} * ([C3_{tot}] - [C3]) + k_{C1} * \frac{[C1]^{n_{17}}}{[C1]^{n_{17}} + J_C^{n_{17}}} * ([C3_{tot}] - [C3]) - k_{dC3} * [C3]. \quad (5)$$

The dynamics of caspase-1 that is described by Eq. (1) mainly contains three terms. The first and second terms represent the activation of caspase-1 induced by stimuli and the cleaved GSDMD, respectively. The last term in Eq. (1) corresponds to the degradation/inactivation of caspase-1, while the dynamic behavior of GSDMD is described by two terms as shown in Eq. (2), including the process of caspase-1-activated GSDMD, which is inhibited by caspase-3, and the basal degradation/inactivation

process of GSDMD. As described by Eq. (3), the dynamics of caspase-9 involves the caspase-1-mediated caspase-9 activation and the caspase-3-mediated caspase-9 activation, as well as the caspase-9 degradation/inactivation. For dynamics of caspase-8 in Eq. (4), the first term corresponds to the processes of stimulation-triggered caspase-8 activation that is suppressed by caspase-1, the second and third terms indicate the caspase-8 activation induced by caspase-3 and caspase-1, respectively, and the last term is for caspase-8 degradation/inactivation. Equation (5) is for dynamics of caspase-3, in which the first two terms are caspase-3 activation induced by caspase-8 and caspase-9, respectively, which are also inhibited by GSDMD, and the third and last terms correspond to the caspase-1-mediated caspase-3 activation and caspase-3 degradation/inactivation, respectively.

The time evolution of the cell population N is described by the following equation:

$$\frac{dN}{dt} = k_0 * N - k_{dN} * N * N - k_{NGD} * \frac{[GD]^{n_{18}}}{[GD]^{n_{18}} + J_{NGD}^{n_{18}}} * N - k_{NC3} * \frac{[C3]^{n_{19}}}{[C3]^{n_{19}} + J_{NC3}^{n_{19}}} * N, \quad (6)$$

where the first two terms correspond to the basal cell proliferation and death, respectively.³² The last two terms represent the decrease of cell population induced by GSDMD-mediated pyroptosis and caspase-3-mediated apoptosis. The cell death rate is defined as the ratio of the population of stimulus-induced cell death to the initial population of cells (steady state of non-stimulated cells), which is described by the formula of $(N_{init} - N)/N_{init}$, where N_{init} is the initial population of cells.

The death decision-making regulatory network has 32 kinetic parameters. Parameters in the model are mostly determined by a global optimization method that minimizes the deviation between simulation results and experimental data, and the rest parameters are estimated within a biologically plausible range based on the previous literature.³³ The experimental data are obtained from bone marrow-derived macrophages (BMMs).¹⁷ The deviation is characterized with the correlation coefficient, R-square, which is determined as the following functions:

$$R^2 = 1 - \frac{\sum_{i=1}^n (y_{exp}(t_i) - y_{sim}(t_i))^2}{\sum_{i=1}^n (y_{exp}(t_i) - \bar{y}_{exp})^2}, \quad (7)$$

where $y_{exp}(t_i)$ and $y_{sim}(t_i)$ are experimental data and simulation results of constituents at time t_i , respectively. The total amounts of the constituents are also estimated based on the experimental study.³⁴ All the parameter descriptions and values are elaborated in Table S1 of the [supplementary material](#).

To examine the reliability of the model, simulations were performed to compare with the corresponding experimental data in BMMs.¹⁷ Dynamics of the five constituents and death rates for wild type (WT), GSDMD knockout (GSDMD KO), and caspase-1 knockout (caspase-1 KO) BMMs are presented in [Fig. 1\(b\)](#). For WT BMMs ([Fig. 1\(b\)](#) (i)), and then GSDMD is cleaved and rapidly accumulated [[Fig. 1\(b\)](#) (ii)] to trigger pyroptosis [[Fig. 1\(b\)](#) (vi)], whereas the apoptosis induction constituents, i.e., caspase-8 [[Fig. 1\(b\)](#) (iii)], caspase-9 [[Fig. 1\(b\)](#) (iv)], and caspase-3 [[Fig. 1\(b\)](#) (v)], remain at rather low

levels because of the inhibition effect of GSDMD. For GSDMD KO BMMs (blue lines and points), both caspase-8 [[Fig. 1\(b\)](#) (iii)] and caspase-9 [[Fig. 1\(b\)](#) (iv)] are cleaved by the activated caspase-1, which subsequently cleaves caspase-3 [[Fig. 1\(b\)](#) (v)] to induce apoptosis [[Fig. 1\(b\)](#) (vi)]. Moreover, compared with GSDMD KO, caspase-1 KO in BMMs (green lines and points) induces a delayed response of the apoptosis constituents [[Figs. 1\(b\)](#) (iii)–[1\(b\)](#) (v)], resulting in a slower cell death pattern [[Fig. 1\(b\)](#) (vi)].

Besides the validation of single protein KO cases, the prediction of various double knockout (DKO) cases is also quantitatively supported by recent experimental observations ([Fig. S2](#) in the [supplementary material](#)), such as the cases of GSDMD/caspase-3 DKO [[Fig. S2\(a\)](#) in the [supplementary material](#)], GSDMD/caspase-8 DKO, GSDMD/caspase-9 DKO [[Fig. S2\(b\)](#) in the [supplementary material](#)],¹⁷ and caspase-1/caspase-8 DKO [[Fig. S2\(c\)](#) in the [supplementary material](#)].³⁵ We also validated the model by testing how the cell death pattern responds to various strength of stimulation [[Fig. S2\(d\)](#) in the [supplementary material](#)]. As the results indicated, an increase of the strength of stimulation would trigger the concurrence of apoptosis and pyroptosis [[Fig. S2\(e\)](#) in the [supplementary material](#)], which is in line with the data obtained in two typical cell lines.³⁶ As a result, the excellent fitting between the simulation and experiment [[Fig. 1\(c\)](#)] indicates that our model has high confidence for further clarifying the underlying mechanisms of death decision-making between pyroptosis and apoptosis.

Sensitivity analysis of the crosstalk in switching cell death modes

In this section, sensitivity analysis is performed to dissect whether and how the components mediate the cell death modes. We first explored the effects of expression levels of the five constituents ($C1_{tot}$, GD_{tot} , $C9_{tot}$, $C8_{tot}$, and $C3_{tot}$) on the death mode switching [[Fig. 2\(a\)](#)]. The sensitivities of the activated caspase-3 (apoptosis effector protein) and the cleaved GSDMD (pyroptosis effector protein) to the change of each component are investigated. We varied the level of each constituent individually in a range from 0.01-fold to 100-fold of its standard value to inquire the activation of caspase-3 and GSDMD. As shown in [Fig. 2\(a\)](#), the 100-fold increase of the five constituent levels from their standard value (i.e., 1-fold) barely affects the activation of caspase-3 [[Fig. 2\(a\)](#) (i)] and GSDMD [[Fig. 2\(a\)](#) (ii)]. However, the decrease of the caspase-1 ($C1_{tot}$) or GSDMD (GD_{tot}) expression level enhances the caspase-3 activation and restrains the GSDMD activation, presenting a death mode switching from pyroptosis to apoptosis, while the decrease of the other three constituents ($C9_{tot}$, $C8_{tot}$, and $C3_{tot}$) barely affects cell death modes. The two-dimensional heat map is presented in the sub-figures of [Fig. 2\(a\)](#). These simulation results are consistent with the experimental observations that GSDMD is essential for pyroptosis induction,¹⁷ and the cell death mode switches from pyroptosis to apoptosis in GSDMD KO or caspase-1 KO cells [[Fig. 1\(b\)](#) (vi)].

There are totally 21 biochemical reactions in the model, which are described by 32 kinetic parameters within a biologically plausible range.³⁷ We next explored the key reactions that can efficiently switch the death modes. The parameter sensitivity analysis indicates that only eight parameter variations can efficiently change the cell death mode between pyroptosis and apoptosis [[Figs. 2\(b\)](#) and [2\(c\)](#)].

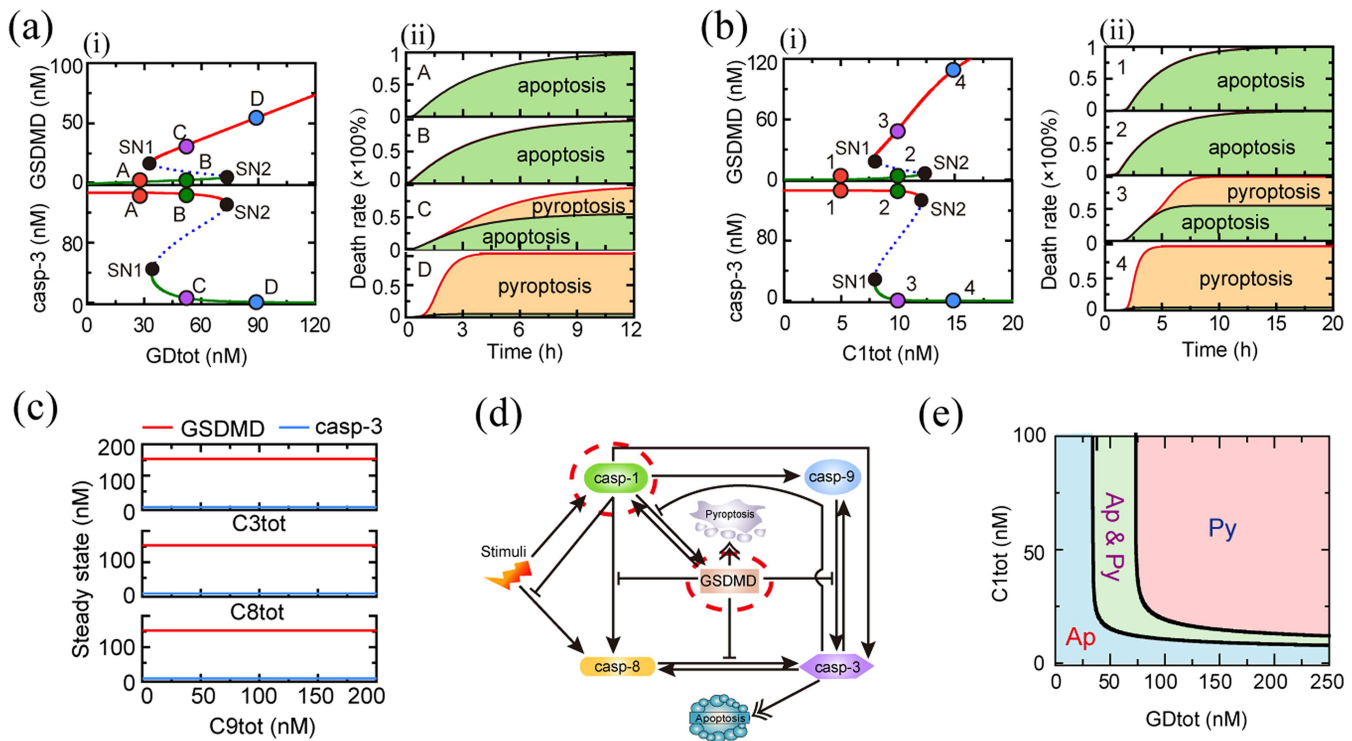


FIG. 3. Role of constituent levels in death mode switching. Bifurcation diagrams of caspase-3 and GSDMD as a function of GDtot (a) (i) and C1tot (b) (i). Stable and unstable steady states are indicated by solid and dashed lines, respectively. (a) (ii) and (b) (ii) reflect the contribution proportions of pyroptosis (brown area) and apoptosis (green area) to cell death for points A–D and 1–4, respectively. (c) Bifurcation diagrams of caspase-3 and GSDMD as functions of C3tot, C8tot, and C9tot. (d) Summary of the constituents that can switch cell death modes. (e) Phase diagram of death modes in response to the variation of caspase-1 (C1tot) and GSDMD (GDtot) expression levels. The green area corresponds to the concurrence of pyroptosis and apoptosis (bistability), while red and blue areas correspond to pyroptosis only and apoptosis only (monostability) modes, respectively.

GDtot = 50 nM), the two stable states are given (point B and point C) [Fig. 3(a) (i)]. The system stable state is sensitive to the initial condition of the activated caspase-3. A small perturbation of caspase-3 will drive the system to one of the two stable states. For example, a small amount of 0.1 nM caspase-3 will converge the system to the stable state with a high level of caspase-3 and a low level of GSDMD [Fig. 3(a) (i), point B], resulting in apoptosis (Fig. 3(a) (ii), point B). However, when the initial condition of the caspase-3 level is zero, the system will converge to the stable state with a comparatively low level of caspase-3 and a high level of GSDMD [Fig. 3(a) (i), point C], inducing the concurrence of pyroptosis and apoptosis [Fig. 3(a) (ii), point C]. When the GSDMD level is high enough (>~75 nM) [Fig. 3(a) (i)], the system presents monostability and the stable state presents a high level of the cleaved GSDMD, which increases with the increase of the GSDMD expression level, while caspase-3 remains at a low value. As the example of point D presented, cells exclusively undergo pyroptosis [Fig. 3(a) (ii)]. Time courses of the four representative points are correspondingly presented in Fig. S3(a) (i) of the [supplementary material](#).

Therefore, these results indicate that the GSDMD expression level is vital for cell death mode switching among various types,

including apoptosis or pyroptosis alone, or the concurrence of apoptosis and pyroptosis. The simulation results are qualitatively supported by the experimental observations that pyroptosis occurs in cells with a high GSDMD level expression, such as macrophage and the small intestine in mice, while apoptosis occurs in cells with a low GSDMD level, for example, spinal cord and L929 cells.¹⁷

Similarly, the effects of the caspase-1 expression level on cell death modes are discussed. As given in Fig. 3(b) (i), with a low level of the caspase-1 expression (<~7.5 nM), apoptosis occurs alone [Fig. 3(b) (ii)], while two steady states are observed with the caspase-1 expression ranging from 7.5 to 12.5 nM. Cells will selectively execute apoptosis alone (Point 2) or the concurrence of apoptosis and pyroptosis (Point 3) depending on its initial conditions. A high expression level of caspase-1 (>~12.5 nM) will induce pyroptosis alone (Point 4). As a result, caspase-1 can also act as a death mode switching factor in cells.

Moreover, according to the bifurcation diagram shown in Fig. 3(c), variation of caspase-3/8/9 expression levels can hardly influence the high value of the steady state of the cleaved GSDMD (red lines) and the low value of the steady state of the activated caspase-3 (blue lines) in cells. Overall, these results suggest that only GSDMD and caspase-1 expression levels are capable to switch

death modes between pyroptosis and apoptosis, while the other three constituents, i.e., caspase-3/8/9, cannot alone [Fig. 3(d)].

A more holistic view on the cell death mode switching with respect to GSDMD and caspase-1 expression levels can be characterized by the phase diagram in the plane of these two constituent expression levels.^{41,42} The phase diagram shown in Fig. 3(e) explicitly presents the distribution of three death modes, i.e., apoptosis only (blue area, monostability), pyroptosis only (red area, monostability), and the concurrence of pyroptosis and apoptosis (green area, bistability). The varying caspase-1 level only triggers apoptosis with a low level of GSDMD (e.g., 15 nM) [Fig. S3(b) in the [supplementary material](#), upper panel] but can induce death mode switching from apoptosis to the concurrence of pyroptosis and apoptosis at a middle GSDMD level (e.g., 50 nM). The three death modes, i.e., apoptosis only, the concurrence of pyroptosis and apoptosis, and

pyroptosis only, can be observed with varying caspase-1 levels at a high GSDMD level (e.g., 100 nM). Similar bifurcation patterns are also observed for the system with varying GSDMD levels [Fig. S3(b) (ii) in the [supplementary material](#), down panel]. Hence, the three death mode switching occurs with different GSDMD and caspase-1 expression levels.

Bifurcation analysis of the reaction in switching death modes

Having dissected the vital constituents, we next focused on exploring whether and how the reactions in the system control cell death modes.^{38,43,44} There are 21 reactions described by 32 kinetic parameters in the system. Bifurcation diagrams of cleaved GSDMD and activated caspase-3 as a function of the activation rate

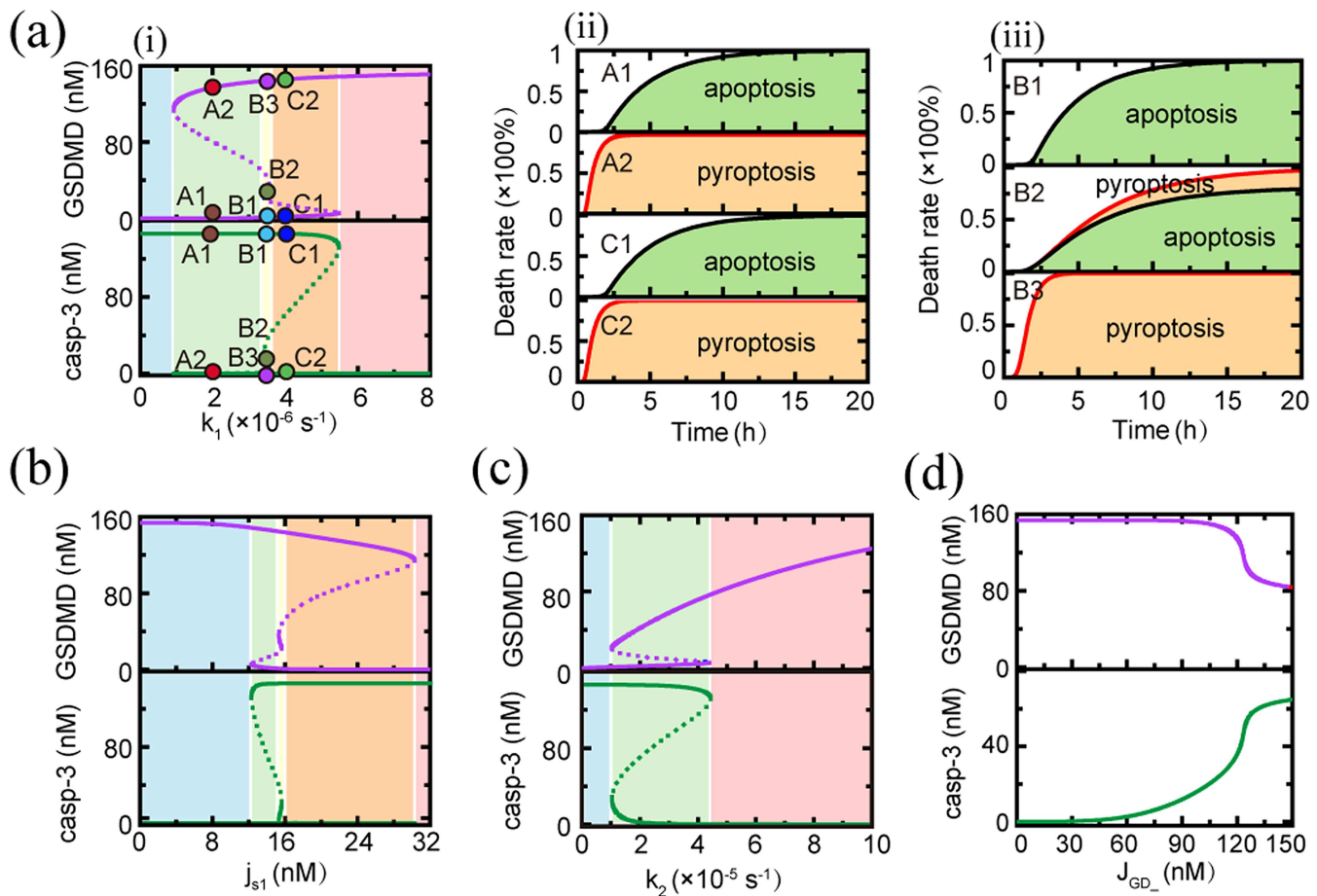


FIG. 4. Role of reaction parameters in death mode switching. (a) (i) Bifurcation diagrams of caspase-3 and GSDMD as a function of the activation rate of caspase-1 induced by stimuli (k_1). (a) (ii) Death mode and death rate of the four representative points (A1, A2, C1, and C2) in the bistable region. (a) (iii) Death rate of the three representative points (B1, B2, and B3) in the tristable region. (b)–(d) Bifurcation diagrams of caspase-3 and GSDMD as a function of the parameters, j_{s1} (Hill-parameter of stimulus-induced caspase-1 activation), k_2 (activation rate of GSDMD induced by caspase-1), and J_{GD-} (Hill-parameter of caspase-8-dependent caspase-3 activation inhibited by GSDMD), that can generate tristability (b), bistability (c), and monostability (d) for death mode switching. Stable and unstable steady states are denoted by solid and dashed lines, respectively.

of caspase-1 induced by stimuli, i.e., parameter k_1 , are shown in Fig. 4(a) (i), presenting five different dynamical regions. A small activation rate of caspase-1 induced by stimuli triggers apoptosis alone (blue region). Then, the increase of k_1 first converges the system to a bistable region (green region) with the occurrence of apoptosis (point A1) or pyroptosis (point A2) [Fig. 4(a) (ii)]. Unexpectedly, the system turns to a tristable range (yellow range) with a further increase of k_1 . The death rates of three examples within the tristable range are shown in Fig. 4(a) (iii), where B1 and B3 correspond to apoptosis only and pyroptosis alone, respectively. However, for B2, both the cleaved GSDMD and the activated caspase-3 remain at relatively low levels, leading to the concurrence of apoptosis and pyroptosis. The system will converge to a bistable state (brown range) and a monostable state (pink range) with further increasing k_1 [Fig. 4(a) (i)]. Time courses of the seven representative points are correspondingly presented in Fig. S4(a) of the supplementary material. Thus, the activation rate of caspase-1 induced by stimuli can drive the system to the monostable, bistable, or tristable state, resulting in diverse death modes.

Bifurcation analysis with all the other reaction parameters in the system are further performed to explore their modulation in death mode switching. After scanning all the 32 reaction parameters, only parameters k_1 and j_{s1} for caspase-1 activation induced by stimuli can induce the tristable state in the system. The bifurcation diagram as a function of j_{s1} also exhibits five dynamical regions, including the monostable, bistable, and tristable states [Fig. 4(b)]. Moreover, only the seven parameters, i.e., the activation rate of GSDMD induced by caspase-1 (k_2), the Hill-parameter of GSDMD activation by caspase-1 (J_{C1}), the Hill-parameter of caspase-3 inhibition by GSDMD (J_{GD}), the Hill-parameter of GSDMD inhibition by caspase-3 (J_{C3}), and the degradation rates of caspase-1 (k_{dC1}),

caspase-3 (k_{dC3}), and GSDMD (k_{dGD}), can generate a bistable state in the system [Figs. 4(c) and S4(b) in the supplementary material] with the other parameters at the standard values.

When changing the other parameters only, the bifurcation diagrams typically present a monostable state for the model with the other parameters at the standard values [Figs. 4(d) and S5 in the supplementary material]. Among those parameters that present monostability, two parameters (J_{GD} and k_{C1}) can efficiently switch the cell death modes. The increase of J_{GD} (parameter of caspase-3 inhibition by GSDMD) or k_{C1} (rate of caspase-3 activated by caspase-1) converges the cell from pyroptosis to the concurrence of apoptosis and pyroptosis [Figs. 4(d) and S4(b) in the supplementary material]. Taken together, only the above mentioned 11 parameters, which correspond to 9 biochemical reactions in the network, can efficiently switch cell death modes.

Effects of constituent levels and reactions on the diverse stable states

The bifurcation diagram is to discuss the effects of a single reaction parameter on the system dynamics with all the other parameters at the standard value, while the phase diagram can display the synergistic modulation of two parameters on the death mode switching.^{45,46} Figure 5(a) shows the distribution of stable states with respect to different GSDMD expression levels and varying activation rates of caspase-1 induced by stimuli (k_1). The diverse stable state variations under four typical GSDMD levels are presented in Fig. S6 of the supplementary material. With a low level of the GSDMD expression, a monostable state for apoptosis occurs alone [Fig. S6(a) (i) in the supplementary material]. A middle level of GSDMD induces the death mode switching from

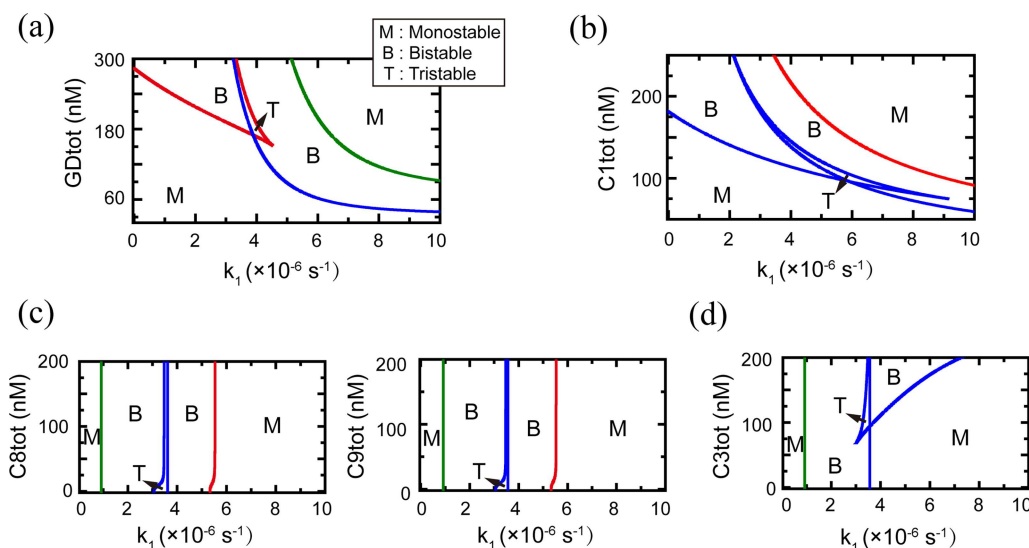


FIG. 5. Effects of constituents on the k_1 (activation rate of caspase-1 induced by stimuli) mediated multistability. The stability distributions of parameters k_1 under various expression levels of GSDMD (a), caspase-1 (b), caspase-8/9 (c), and caspase-3 (d), respectively. M, B, and T, respectively, correspond to the range of monostable, bistable, and tristable.

monostable apoptosis to bistable states of apoptosis and pyroptosis and then to monostable pyroptosis [Fig. S6(a) (ii) in the [supplementary material](#)]. Besides, the state change from monostability to tristability, to bistability, and then to monostability can be observed with a high GSDMD expression [Fig. S6(a) (iii) in the [supplementary material](#)]. A higher level of GSDMD induces the switch from bistability to tristability, to bistability, and finally to monostability [Fig. S6(a) (iv) in the [supplementary material](#)].

Moreover, the phase diagram with respect to the caspase-1 expression level and the activation rate of caspase-1 induced by stimuli (k_1) is shown in Fig. 5(b). Similar to GSDMD, a low level of caspase-1 only induces monostable apoptosis, while high levels can trigger the changes between various stable states [Fig. S5(b) in the [supplementary material](#)]. Besides GSDMD and caspase-1, we further tested the state distribution with respect to caspase-3/8/9. The changes of the expression levels of caspase-8/9 have little influence on the change of cell death modes [Fig. 5(c)], which is different from the effect of caspase-3 [Fig. 5(d)].

We further explored the synergistic effects of the co-variation of parameter k_1 and any one of the four key reaction rates (k_2 , J_{GD} , J_{C3i} , and J_{GD-}) that trigger bistability or monostability [Figs. 4(c) and S4(b) in the [supplementary material](#)] on the death mode switching. The corresponding phase diagrams are shown in Fig. 6. Compared with the other three parameters (k_2 , J_{C3i} , and J_{GD}) [Figs. 6(a)–6(c)], two tristable areas are observed in the phase diagram for J_{GD-} and k_1 [Fig. 6(d)], suggesting a complicated role of J_{GD-} in determining

the diverse cell death modes. Besides, the phase diagrams for k_1 with other parameters that trigger monostability but cannot switch death modes (Fig. S5 in the [supplementary material](#)), such as the caspase-8 inhibition by caspase-1 (j_{C1}) and the caspase-8 inhibition by GSDMD (j_{GD1}), indicate that these parameters barely influence the k_1 -mediated stable state switching [Figs. 6(e)–6(f) and S7 in the [supplementary material](#)].

DISCUSSION

Although most studies so far have concentrated on the molecular mechanisms of various types of cell death, emerging evidence suggests the intricate crosstalk of different cell death pathways.^{47,48} Dissecting how these pathways synergistically work together to generate specific cell fate decision is an important question.^{2,48,49} During the last several years, a rich body of studies have determined the essential function of the gasdermin family in pyroptosis and its crosstalk with apoptosis.^{9,17,18} Taken together with these experimental observations, we constructed a simplified cell death crosstalk model. We aimed to reveal the regulatory mechanisms of the crosstalk between pyroptotic and apoptotic pathways, highlighting the phase diagram of various death modes in different parameter spaces.

Both approaches of sensitivity analysis and bifurcation analysis are performed to expose the components that can efficiently switch cell death modes.^{38,39,46} The deterministic interactions for cell

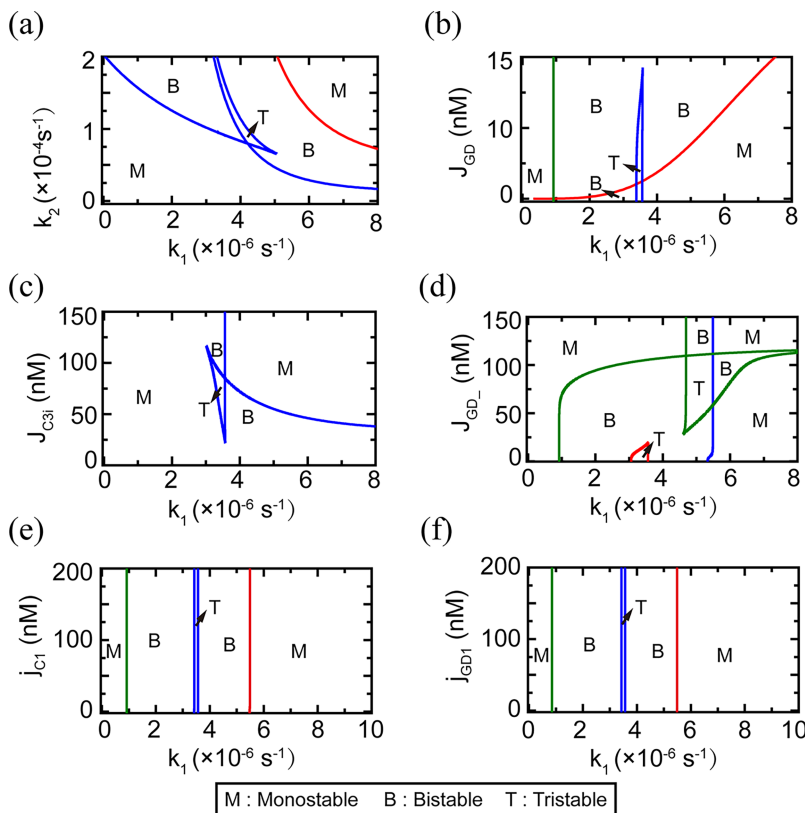


FIG. 6. Effects of crucial reactions on the k_1 (activation rate of caspase-1 induced by stimuli) mediated multistability. (a)–(c) Phase diagram of the system stability on parameters k_1 with respect to the three parameters, k_2 (caspase-1-dependent activation rate of GSDMD), J_{GD} (Hill-parameter of caspase-9-dependent caspase-3 activation inhibited by GSDMD), and J_{C3i} (Hill-parameter of GSDMD inhibition by caspase-3), that trigger bistability. (d) Phase diagram of the system stability on parameters k_1 with respect to the parameter J_{GD-} (Hill-parameter of caspase-8-dependent caspase-3 activation inhibited by GSDMD) that trigger monostability for death mode switching. (e)–(f) denote the stability distributions of parameters k_1 with respect to the parameters, j_{C1} (Hill-parameter of caspase-8 inhibition by caspase-1) and j_{GD1} (Hill-parameter of caspase-8 inhibition by GSDMD), that cannot switch death modes. M, B, and T, respectively, correspond to the range of monostable, bistable, and tristable.

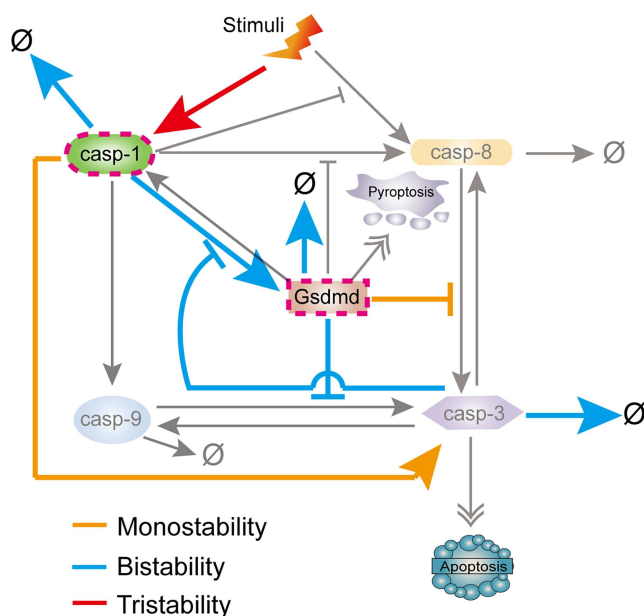


FIG. 7. Summary of the components that can switch cell death modes. Variations of the two constituents (caspase-1 and GSDMD) and nine reactions that can change death modes between pyroptosis and apoptosis are colored. The red, blue, and yellow lines represent the reactions that can trigger tristability, bistability, and monostability for switching death modes, respectively.

death mode switching are then obtained, as shown in Fig. 7. The two approaches severally indicate that only the level of caspase-1 or GSDMD can individually cause a cell death switch between pyroptosis and apoptosis, which are supported by the experimental observations.¹⁷ We also predict that varying the levels of caspase-3/8/9 cannot change the death mode of pyroptosis, which need to be further validated by experiments.

Sensitivity analysis ascertains that eight parameters can switch cell death modes. However, 11 parameters that correspond to 9 biochemical reactions (Fig. 7) are determined for cell death mode switching by bifurcation analysis. As a result, we determine the nine key reactions among totally 21 reactions in the crosstalk to switch death modes among monostability, bistability, and tristability states. The predicted multistability elucidates the mechanistic basis of various switches between pyroptosis and apoptosis, which need to be further experimentally validated.

In accordance with a very recently experimental study of caspase-1,^{9,17,18,50,51} our study demonstrated that caspase-1 is a central signaling node for determining the cell fate between pyroptosis and apoptosis. As shown in Fig. 7, besides the level of caspase-1, five of the nine identified key reactions are directly related to caspase-1. Actually, caspase-1 can initiate both the pyroptotic and apoptotic pathways. A high level of caspase-1 induces pyroptosis, while a low level leads to apoptosis [Fig. 3(b)]. Importantly, our study indicates that caspase-1 has the potential to simultaneously cause the occurrence of pyroptosis and apoptosis. There are two types of co-occurrence of pyroptosis and apoptosis predicted by our bifurcation

analysis. One appears within the bistable range [Fig. 3(b) (ii), point 3), and the other is induced within the tristable range [Fig. 4(a) (iii), point B2). Besides the exclusive occurrence of apoptosis and pyroptosis, we thus hypothesize the existence of the mixed death mode that apoptosis and pyroptosis can simultaneously occur in individual cells. Besides, the two-parameter bifurcation analysis shows a more global view of multistability. The various cell fate states unveil the possible molecular mechanisms in pathological cells.

As a type of inflammatory cell death, pyroptosis plays diverse roles in various diseases. Inducing pyroptosis can efficiently block the growth, proliferation, and invasion of tumor cells.⁵² However, excessive pyroptosis can also incur autoimmune diseases (such as systemic lupus erythematosus), neurodegenerative diseases (such as Alzheimer's disease), cardiovascular disease (such as cerebral ischemia), and even metabolic diseases (such as atherosclerosis)^{53,54} due to the release of cytokines (such as IL-1 β and IL-18) and cellular contents that have toxic effects.⁵⁵ Thus, as pointed out by our study, focusing on exploring the efficient control strategy of the levels of caspase-1 and GSDMD is an urgent issue. Actually, biologists have developed several caspase-1/GSDMD inhibitor drugs for disease treatment in recent years. The structure-based discovery of 3-[3-(thiophene-2-carboxamido)benzamido]benzoic acid (CZL80) offers much therapeutic potential for febrile seizures via inhibiting the level of caspase-1.⁵⁶ Necrosulfonamide, a newly found chemical inhibitor of GSDMD, can directly bind GSDMD to cause the decrease of cleaved GSDMD, resulting in the inhibition of pyroptosis.⁵⁷ Valbopropo, an inhibitor of dipeptidyl peptidase 8/9 (DPP8/DPP9), can promote the activation of caspase-1 to treat acute myeloid leukemia through inducing pyroptosis.^{58,59} Besides, 2-4-diaminopyrimidine, an important fragment in the inhibition of human caspase-1, is designed to be applied for the treatment of Alzheimer's disease.^{60,61} Although there is no direct evidence right now to support our predictions, these results at least highlight the dynamical regulatory mechanism of the functional components in the network for various state transitions, which offer the theoretical guidance of drug development for the treatment of pyroptosis-related diseases in the future.

SUPPLEMENTARY MATERIAL

A detailed overview of the crosstalk between pyroptotic and apoptotic signaling network and the corresponding supplementary figures/table are presented in the [supplementary material](#).

AUTHORS' CONTRIBUTIONS

Z.Y. and P.-p.Z. conceptualized the study. Z.Y., P.-p.Z., X.L., and J.J. developed the models and performed simulations. F.X., Z.L., L.Z., and H.Q. helped to analyze data. Z.Y., J.S., and X.L. wrote the paper. Z.Y. and P.-p.Z. contributed equally to this work.

ACKNOWLEDGMENTS

This work was supported by the National Natural Science Foundation of China (NNSFC) (Grant Nos. 12090052 and 11874310), the China Postdoctoral Science Foundation (Grant No. 2016M602071), and the Shanxi Province Science Foundation for Youths (Grant No. 201901D211159).

DATA AVAILABILITY

The ODE model is developed and simulated with MATLAB, and the ode 15s function of MATLAB is used to solve ODEs. Zipped mathematical code files of the model to generate the results in this study are available from the corresponding authors upon reasonable request.

REFERENCES

- ¹N. M. de Vasconcelos and M. Lamkanfi, "Recent insights on inflammasomes, gasdermin pores, and pyroptosis," *Cold Spring Harb. Perspect. Biol.* **12**(5), a036392 (2020).
- ²X. Xia, X. Wang, Z. Cheng, W. Qin, L. Lei, J. Jiang, and J. Hu, "The role of pyroptosis in cancer: Pro-cancer or pro-host?," *Cell Death Dis.* **10**, 650 (2019).
- ³P. Broz and V. M. Dixit, "Inflammasomes: Mechanism of assembly, regulation and signalling," *Nat. Rev. Immunol.* **16**(7), 407–420 (2016).
- ⁴H. T. H. Thi and S. Hong, "Inflammasome as a therapeutic target for cancer prevention and treatment," *J. Cancer Prev.* **22**(2), 62–73 (2017).
- ⁵T. Bergsbaken, S. L. Fink, and B. T. Cookson, "Pyroptosis: Host cell death and inflammation," *Nat. Rev. Microbiol.* **7**(2), 99–109 (2009).
- ⁶C. Yu, J. Moeking, M. Geyer, and S. L. Masters, "Mechanisms of NLRP1-mediated autoinflammatory disease in humans and mice," *J. Mol. Biol.* **430**(2), 142–152 (2018).
- ⁷K. W. Chen, B. Demarco, and P. Broz, "Beyond inflammasomes: Emerging function of gasdermins during apoptosis and NETosis," *EMBO J.* **39**(2), e103397 (2020).
- ⁸F. Martinon, K. Burns, and J. Tschopp, "The inflammasome: A molecular platform triggering activation of inflammatory caspases and processing of proIL-beta," *Mol. Cell* **10**(2), 417–426 (2002).
- ⁹W. He, H. Wan, L. Hu, P. Chen, X. Wang, Z. Huang, Z. Yang, C. Zhong, and J. Han, "Gasdermin D is an executor of pyroptosis and required for interleukin-1 beta secretion," *Cell Res.* **25**(12), 1285–1298 (2015).
- ¹⁰N. Kayagaki, I. B. Stowe, B. L. Lee, K. O'Rourke, K. Anderson, S. Warming, T. Cuellar, B. Haley, M. Roose-Girma, Q. T. Phung, P. S. Liu, J. R. Lill, H. Li, J. Wu, S. Kummerfeld, J. Zhang, W. P. Lee, S. J. Snipas, G. S. Salvesen, L. X. Morris, L. Fitzgerald, Y. Zhang, E. M. Bertram, C. C. Goodnow, and V. M. Dixit, "Caspase-11 cleaves gasdermin D for non-canonical inflammasome signalling," *Nature* **526**(7575), 666–671 (2015).
- ¹¹J. Shi, Y. Zhao, K. Wang, X. Shi, Y. Wang, H. Huang, Y. Zhuang, T. Cai, F. Wang, and F. Shao, "Cleavage of GSDMD by inflammatory caspases determines pyroptotic cell death," *Nature* **526**(7575), 660–665 (2015).
- ¹²S. B. Kovacs and E. A. Miao, "Gasdermins: Effectors of pyroptosis," *Trends Cell Biol.* **27**(9), 673–684 (2017).
- ¹³P. Orning, E. Lien, and K. A. Fitzgerald, "Gasdermins and their role in immunity and inflammation," *J. Exp. Med.* **216**(11), 2453–2465 (2019).
- ¹⁴P. Broz, J. von Moltke, J. W. Jones, R. E. Vance, and D. M. Monack, "Differential requirement for caspase-1 autoproteolysis in pathogen-induced cell death and cytokine processing," *Cell Host Microbe* **8**(6), 471–483 (2010).
- ¹⁵S. Bedoui, M. J. Herold, and A. Strasser, "Emerging connectivity of programmed cell death pathways and its physiological implications," *Nat. Rev. Mol. Cell Biol.* **21**(11), 678–695 (2020).
- ¹⁶X. Li, C. Zhong, R. Wu, X. Xu, Z. Yang, S. Cai, X. Wu, X. Chen, Z. Yin, Q. He, D. Li, F. Xu, Y. Yan, H. Qi, C. Xie, J. Shuai, and J. Han, "RIP1-dependent linear and nonlinear recruitments of caspase-8 and RIP3 respectively to necrosome specify distinct cell death outcomes," *Protein Cell* **1–19** (2021).
- ¹⁷K. Tsuchiya, S. Nakajima, S. Hosojima, D. Thi Nguyen, T. Hattori, T. Manh Le, O. Hori, M. R. Mahib, Y. Yamaguchi, M. Miura, T. Kinoshita, H. Kushiya, M. Sakurai, T. Shiroishi, and T. Suda, "Caspase-1 initiates apoptosis in the absence of gasdermin D," *Nat. Commun.* **10**, 2091 (2019).
- ¹⁸C. Y. Taabazuing, M. C. Okondo, and D. A. Bachovchin, "Pyroptosis and apoptosis pathways engage in bidirectional crosstalk in monocytes and macrophages," *Cell Chem. Biol.* **24**(4), 507–514 (2017).
- ¹⁹C. Rogers, T. Fernandes-Alnemri, L. Mayes, D. Alnemri, G. Cingolani, and E. S. Alnemri, "Cleavage of DFNA5 by caspase-3 during apoptosis mediates progression to secondary necrotic/pyroptotic cell death," *Nat. Commun.* **8**, 14128 (2017).
- ²⁰C. Rogers, D. A. Erkes, A. Nardone, A. E. Aplin, T. Fernandes-Alnemri, and E. S. Alnemri, "Gasdermin pores permeabilize mitochondria to augment caspase-3 activation during apoptosis and inflammasome activation," *Nat. Commun.* **10**, 1689 (2019).
- ²¹J. Sarhan, B. C. Liu, H. I. Muendlein, P. Li, R. Nilson, A. Y. Tang, A. Rongvaux, S. C. Bunnell, F. Shao, D. R. Green, and A. Poltorak, "Caspase-8 induces cleavage of gasdermin D to elicit pyroptosis during yersinia infection," *Proc. Natl. Acad. Sci. U.S.A.* **115**(46), E10888–E10897 (2018).
- ²²P. Orning, D. Weng, K. Starheim, D. Ratner, Z. Best, B. Lee, A. Brooks, S. Xia, H. Wu, M. A. Kelliher, S. B. Berger, P. J. Gough, J. Bertin, M. M. Proulx, J. D. Goguen, N. Kayagaki, K. A. Fitzgerald, and E. Lien, "Pathogen blockade of TAK1 triggers caspase-8-dependent cleavage of gasdermin D and cell death," *Science* **362**(6418), 1064–1069 (2018).
- ²³K. W. Chen, B. Demarco, R. Heilig, K. Shkarina, A. Boettcher, C. J. Farady, P. Pelczar, and P. Broz, "Extrinsic and intrinsic apoptosis activate pannexin-1 to drive NLRP3 inflammasome assembly," *EMBO J.* **38**(10), e101638 (2019).
- ²⁴H. Qi, X. Li, Z. Jin, T. Simmen, and J. Shuai, "The oscillation amplitude, not the frequency of cytosolic calcium, regulates apoptosis induction," *iScience* **23**(11), 101671 (2020).
- ²⁵X. Li, C. Zhong, Z. Yin, H. Qi, F. Xu, Q. He, and J. Shuai, "Data-driven modeling identifies TRAP-independent MyD88 activation complex and myddosome assembly strategy in LPS/TLR4 signaling," *Int. J. Mol. Sci.* **21**(9), 3061 (2020).
- ²⁶Y. Bi, Z. Yang, C. Zhuge, and J. Lei, "Bifurcation analysis and potential landscapes of the p53-Mdm2 module regulated by the co-activator programmed cell death," *Chaos* **25**(11), 113103 (2015).
- ²⁷S. Rühl and P. Broz, "Caspase-11 activates a canonical NLRP3 inflammasome by promoting K⁺ efflux," *Eur. J. Immunol.* **45**(10), 2927–2936 (2015).
- ²⁸N. Van Opendenbosch, H. Van Gorp, M. Verdonck, P. H. V. Saavedra, N. M. de Vasconcelos, A. Goncalves, L. Vande Walle, D. Demon, M. Matusiak, F. Van Hauwermeiren, J. D'Hont, T. Hochepeid, S. Krautwald, T.-D. Kanneganti, and M. Lamkanfi, "Caspase-1 engagement and TLR-induced c-FLIP expression suppress ASC/caspase-8-dependent apoptosis by inflammasome sensors NLRP1 and NLR4," *Cell Rep.* **21**(12), 3427–3444 (2017).
- ²⁹X. Cheng and J. E. Ferrell, "Apoptosis propagates through the cytoplasm as trigger waves," *Science* **361**(6402), 607–612 (2018).
- ³⁰M. W. Anderson, J. J. Moss, R. Szalai, and J. D. Lane, "Mathematical modeling highlights the complex role of AKT in TRAIL-induced apoptosis of colorectal carcinoma cells," *iScience* **12**, 182–193 (2019).
- ³¹E. Z. Bagci, Y. Vodovotz, T. R. Billiar, G. B. Ermentrout, and I. Bahar, "Bistability in apoptosis: Roles of Bax, Bcl-2, and mitochondrial permeability transition pores," *Biophys. J.* **90**(5), 1546–1559 (2006).
- ³²D. A. Charlebois and G. Balazsi, "Modeling cell population dynamics," *In Silico Biol.* **13**(1–2), 21–39 (2018).
- ³³J. G. Albeck, J. M. Burke, S. L. Spencer, D. A. Lauffenburger, and P. K. Sorger, "Modeling a snap-action, variable-delay switch controlling extrinsic cell death," *PLoS Biol.* **6**(12), e299 (2008).
- ³⁴B. Schwanhaeusser, D. Busse, N. Li, G. Dittmar, J. Schuchhardt, J. Wolf, W. Chen, and M. Selbach, "Global quantification of mammalian gene expression control," *Nature* **473**(7347), 337–342 (2011).
- ³⁵S. Christgen, M. Zheng, S. Kesavardhana, R. Karki, R. K. S. Malireddi, B. Banoth, D. E. Place, B. Briard, B. R. Sharma, S. Tuladhar, P. Samir, A. Burton, and T.-D. Kanneganti, "Identification of the PANoptosome: A molecular platform triggering pyroptosis, apoptosis, and necroptosis (PANoptosis)," *Front. Cell. Infect. Microbiol.* **10**, 237 (2020).
- ³⁶F. Y. Mai, P. He, J. Z. Ye, L. H. Xu, D. Y. Ouyang, C. G. Li, Q. Z. Zeng, C. Zeng, C. Y. Zeng, C. C. Zhang, X. H. He, and B. Hu, "Caspase-3-mediated GSDME activation contributes to cisplatin- and doxorubicin-induced secondary necrosis in mouse macrophages," *Cell Prolif.* **52**(5), e12663 (2019).
- ³⁷W. Ma, A. Trusina, H. El-Samad, W. A. Lim, and C. Tang, "Defining network topologies that can achieve biochemical adaptation," *Cell* **138**(4), 760–773 (2009).
- ³⁸L. Zhao, T. Sun, J. Pei, and Q. Ouyang, "Mutation-induced protein interaction kinetics changes affect apoptotic network dynamic properties and facilitate oncogenesis," *Proc. Natl. Acad. Sci. U.S.A.* **112**(30), E4046–E4054 (2015).

- ³⁹Y. Zhao, D. D. Wang, Z. W. Zhang, Y. Lu, X. J. Yang, Q. Ouyang, C. Tang, and F. T. Li, "Critical slowing down and attractive manifold: A mechanism for dynamic robustness in the yeast cell-cycle process," *Phys. Rev. E* **101**(4), 042405 (2020).
- ⁴⁰J. E. Ferrell and W. Xiong, "Bistability in cell signaling: How to make continuous processes discontinuous, and reversible processes irreversible," *Chaos* **11**(1), 227–236 (2001).
- ⁴¹D. Jia, M. K. Jolly, W. Harrison, M. Boareto, E. Ben-Jacob, and H. Levine, "Operating principles of tristable circuits regulating cellular differentiation," *Phys. Biol.* **14**(3), 035007 (2017).
- ⁴²J. Zhu, "Unified mechanism of inverse stochastic resonance for monostability and bistability in Hindmarsh-Rose neuron," *Chaos* **31**(3), 033119 (2021).
- ⁴³X. Tian, H. Zhang, and J. Xing, "Coupled reversible and irreversible bistable switches underlying TGF beta-induced epithelial to mesenchymal transition," *Biophys. J.* **105**(4), 1079–1089 (2013).
- ⁴⁴Z. Yin, H. Qi, L. Liu, and Z. Jin, "The optimal regulation mode of Bcl-2 apoptotic switch revealed by bistability analysis," *Biosystems* **162**, 44–52 (2017).
- ⁴⁵K. Sathiyadevi, V. K. Chandrasekar, D. V. Senthilkumar, and M. Lakshmanan, "Distinct collective states due to trade-off between attractive and repulsive couplings," *Phys. Rev. E* **97**(3), 032207 (2018).
- ⁴⁶Z. Zhang, Z. Wu, D. Lu, G. Xia, and T. Deng, "Controllable spiking dynamics in cascaded VCSEL-SA photonic neurons," *Nonlinear Dyn.* **99**(2), 1103–1114 (2020).
- ⁴⁷K. Newton, K. E. Wickliffe, A. Maltzman, D. L. Dugger, R. Reja, Y. Zhang, M. Roose-Girma, Z. Modrusan, M. S. Sagolla, J. D. Webster, and V. M. Dixit, "Activity of caspase-8 determines plasticity between cell death pathways," *Nature* **575**(7784), 679–682 (2019).
- ⁴⁸R. Schwarzer, L. Laurien, and M. Pasparakis, "New insights into the regulation of apoptosis, necroptosis, and pyroptosis by receptor interacting protein kinase 1 and caspase-8," *Curr. Opin. Cell Biol.* **63**, 186–193 (2020).
- ⁴⁹R. K. S. Malireddi, P. Gurung, J. Mavuluri, T. K. Dasari, J. M. Klco, H. Chi, and T. Kanneganti, "TAK1 restricts spontaneous NLRP3 activation and cell death to control myeloid proliferation," *J. Exp. Med.* **215**(4), 1023–1034 (2018).
- ⁵⁰J. Li, J. Hao, D. Yao, R. Li, X. Li, Z. Yu, X. Luo, X. Liu, M. Wang, and W. Wang, "Caspase-1 inhibition prevents neuronal death by targeting the canonical inflammasome pathway of pyroptosis in a murine model of cerebral ischemia," *CNS Neurosci. Ther.* **26**(9), 925–939 (2020).
- ⁵¹J. L. Zhang, and K. H. Wei, "Necrosulfonamide reverses pyroptosis-induced inhibition of proliferation and differentiation of osteoblasts through the NLRP3/caspase-1/GSDMD pathway," *Exp. Cell Res.* **405**(2), 112648 (2021).
- ⁵²L. Wang, X. Qin, J. Liang, and P. Ge, "Induction of pyroptosis: A promising strategy for cancer treatment," *Front. Oncol.* **11**, 635774 (2021).
- ⁵³P. Yu, X. Zhang, N. Liu, L. Tang, C. Peng, and X. Chen, "Pyroptosis: Mechanisms and diseases," *Signal Transduct. Target Ther.* **6**, 128 (2021).
- ⁵⁴X. Liu, S. Xia, Z. Zhang, H. Wu, and J. Lieberman, "Channelling inflammation: Gasdermins in physiology and disease," *Nat. Rev. Drug Discov.* **20**(5), 384–405 (2021).
- ⁵⁵J. Tang, M. Bei, J. Zhu, G. Xu, D. Chen, X. Jin, J. Huang, J. Dong, L. Shi, L. Xu, and B. Hu, "Acute cadmium exposure induces GSDME-mediated pyroptosis in triple-negative breast cancer cells through ROS generation and NLRP3 inflammasome pathway activation," *Environ. Toxicol. Pharmacol.* **87**, 103686 (2021).
- ⁵⁶Y. Tang, B. Feng, Y. Wang, H. Sun, Y. You, J. Yu, B. Chen, C. Xu, Y. Ruan, S. Cui, G. Hu, T. Hou, and Z. Chen, "Structure-based discovery of CZL80, a caspase-1 inhibitor with therapeutic potential for febrile seizures and later enhanced epileptogenic susceptibility," *Br. J. Pharmacol.* **177**(15), 3519–3534 (2020).
- ⁵⁷J. K. Rathkey, J. Zhao, Z. Liu, Y. Chen, J. Yang, H. C. Kondolf, B. L. Benson, S. M. Chirieleison, A. Y. Huang, G. R. Dubyak, T. S. Xiao, X. Li, and D. W. Abbott, "Chemical disruption of the pyroptotic pore-forming protein gasdermin D inhibits inflammatory cell death and sepsis," *Sci. Immunol.* **3**(26), eaat2738 (2018).
- ⁵⁸M. C. Okondo, D. C. Johnson, R. Sridharan, E. Bin Go, A. J. Chui, M. S. Wang, S. E. Poplawski, W. Wu, Y. Liu, J. H. Lai, D. G. Sanford, M. O. Arciprete, T. R. Golub, W. W. Bachovchin, and D. A. Bachovchin, "DPP8 and DPP9 inhibition induces pro-caspase-1-dependent monocyte and macrophage pyroptosis," *Nat. Chem. Biol.* **13**(1), 46–53 (2017).
- ⁵⁹D. C. Johnson, C. Y. Taabazuing, M. C. Okondo, A. J. Chui, S. D. Rao, F. C. Brown, C. Reed, E. Peguero, E. de Stanchina, A. Kentsis, and D. A. Bachovchin, "DPP8/DPP9 inhibitor-induced pyroptosis for treatment of acute myeloid leukemia," *Nat. Med.* **24**(8), 1151–1156 (2018).
- ⁶⁰S. Patel, P. Modi, V. Ranjan, and M. Chhabria, "Structure-based design, synthesis and evaluation of 2,4-diaminopyrimidine derivatives as novel caspase-1 inhibitors," *Bioorg. Chem.* **78**, 258–268 (2018).
- ⁶¹R. O. Kumi, O. S. Soremekun, A. R. Issahaku, C. Agoni, F. A. Olotu, and M. E. S. Soliman, "Exploring the ring potential of 2,4-diaminopyrimidine derivatives towards the identification of novel caspase-1 inhibitors in Alzheimer's disease therapy," *J. Mol. Model.* **26**(4), 68 (2020).